CONF-890665--2

COMPOUND-LENS DIODE FOR HERMES III*

T. W. L. Sanford, J. A. Halbleib, J. W. Poukey,
T. Sheridan, D. Muirhead, C. E. Yagow,
K. A. Mikkelson, and R. Mock
Sandia National Laboratories
P. O. Box 5800
Albuquerque, NM 87185

and

P. W. Spence, V. L. Bailey, and H. Kishi
Pulse Sciences, Inc.
600 McCormick St.
San Leandro, CA 94577

SAND--88-3360C

DE89 013065

Abstract

Significantly improved spatial uniformity of bremsstrahlung radiation, relative to a diode with a planar anode, is predicted for the HERMES III accelerator when a compound-lens diode is used to actively control the high-power electron beam at the exit of a coaxial, magnetically-insulated transmission line. Electron flow within the diode and subsequent radiation output is characterized as a function of diode parameters. The results of these calculations are applicable to coaxial geometries where active control of high-energy, high-current, $\nu/\gamma \geq 1$ beams is desired.

Introduction

HERMES III is a 19 ± 2 MV, 700 ± 70 kA electron accelerator designed to produce a uniform source of pulsed γ rays [1]. The source region consists of a 30-Ω, coaxial, MITL (magnetically-insulated transmission line) terminated by a field-emission diode and electron target [2]. In a diode with a planar-anode target and small AK (anode-cathode) gap, the beam forms a weak pinch because the radial electric field is shorted out at the target. This pinch, characterized by the average pinch angle, θ, causes the radiation generated to be focused on axis, which leads to a non-uniform radiation pattern (Figure 1). By extending the AK gap [2] or by indenting the anode near the target [3], the beam can be *passively* controlled to reduce θ, producing a more uniform radiation pattern. For HERMES III parameters, θ can be reduced to about 20° by either method before current losses to the side wall become significant.

This paper discusses the design of an alternative diode configuration, the compound-lens diode, that avoids this limit by *actively* controlling the beam. The concept is illustrated in Figures 2A and B. In this design, the electron beam is incident on a thin, conical-foil window followed by a low-pressure gas cell and bremsstrahlung target. The gas provides rapid charge and current neutralization of the incident beam. When an external current is applied (I_{lens}), a B_θ field is generated. By adjusting the current, the beam can be made to impact the target at the desired small average angle. Because the B_θ field decreases inversely with the radial distance from the axis, the curvature of the trajectories of electrons at smaller radii are greater than that of electrons at larger radii. By angling the entrance foil of the gas cell as shown, the electrons at larger radii remain in the field region longer, and the effect of the decrease in field strength and higher injection angles at large radii is partially compensated. This compensation enables the electrons to impact the target with trajectories nearly parallel to the accelerator axis. This condition of paraxial impact angles ($\theta \approx 0$) approximately optimizes the uniformity of the radiation pattern. Moreover, by orienting the foil as shown, the electrostatic force generated between the conical surface and the beam in the AK gap reduces the pinch angle at the foil. This reduction reduces the external current required to achieve paraxial conditions.

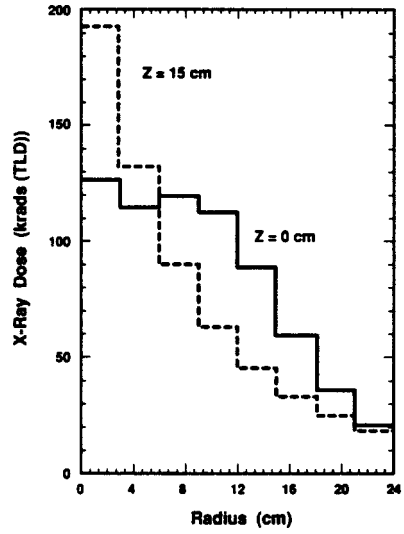

Figure 1. Radiation dose profiles at target face and 15-cm downstream calculated for planar-anode diode having a 50-cm AK gap assuming V(peak) = 18 MV, and Q = 23.2 mC. θ = 32° ± 8°. See Figure 2 for definition of R and Z.

Because of the two-component mechanism for controlling the beam (electrostatic from the orientation of the conical surface [Figure 2A] and magnetic from the external current [Figure 2B]), we call this arrangement the compound lens. The inverse arrangement, with the foil normal to the beam axis and the target conical (B_θ-lens diode), has been successfully tested on the HELIA accelerator operating at 3.2 MV and 150 kA [4].

*This work was supported by the U.S. Department of Energy under Contract DE-AC04-76DP00789.

DISTRIBUTION OF THIS DOCUMENT IS UNLIMITED

MASTER

DISCLAIMER

This report was prepared as an account of work sponsored by an agency of the United States Government. Neither the United States Government nor any agency thereof, nor any of their employees, makes any warranty, express or implied, or assumes any legal liability or responsibility for the accuracy, completeness, or usefulness of any information, apparatus, product, or process disclosed, or represents that its use would not infringe privately owned rights. Reference herein to any specific commercial product, process, or service by trade name, trademark, manufacturer, or otherwise does not necessarily constitute or imply its endorsement, recommendation, or favoring by the United States Government or any agency thereof. The views and opinions of authors expressed herein do not necessarily state or reflect those of the United States Government or any agency thereof.

DISCLAIMER

Portions of this document may be illegible in electronic image products. Images are produced from the best available original document.

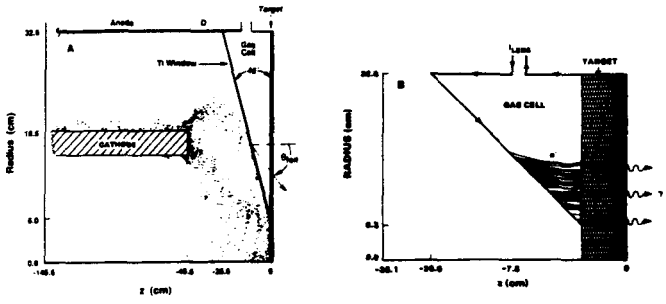

Figure 2(A). MAGIC simulation of electron flow in 20-cm AK gap, and (B) CYLTRAN simulation of electron trajectories in gas cell operating with I_{lens} = 156 kA for the compound-lens diode.

In this paper, the electron flow in the AK gap is simulated using the electromagnetic particle-in-cell computer code, MAGIC [5]. The subsequent electron flow in the gas cell and the electron-photon shower in the target is simulated using the CYLTRAN Monte Carlo code of the ITS system [6]. In the next sections, we discuss in greater detail (I) the characteristics of this flow as a function of AK gap, (II) the characteristics of the resulting radiation pattern as a function of external current, for fixed AK gap, and (III) design considerations.

I. Electron Flow

For AK gaps in excess of about 15 cm, the diode is matched in impedance to the upstream MITL [2]. It is in this line-dominated regime that we operate the diode. Figure 3A shows the characteristic radial current density and angle of incidence at the conical foil calculated for operation in this regime. In the calculation, the AK gap is set to 20 cm. From Figure 3A we see that the peak current density occurs at a radius of 15 cm. The associated angle of incidence is 17.1 $\pm$ 2° and the angle current-averaged over the entire foil is 15° $\pm$ 4.3° (Table 1). Figure 3B shows the resulting radial position and angle of incidence of the beam calculated at the target for an external current of 156 kA, assuming 20 MeV electrons. The current was chosen to turn the beam at a 15-cm radius to normal incidence at the target. From Figure 3B we see that the bulk of the beam is also turned to paraxial trajectories. Specifically, 90% of the beam is contained within the radial range 8 to 22 cm. Over this range, the average systematic variation of the beam is less than $\pm$2°.

As the AK gap is increased, the position of peak current density at the foil and target moves outward, which results in reduced doses over larger areas. Table 1 summarizes the characteristics of the beam at the entrance foil and target for external currents I° required to turn a 20 MeV beam to normal incidence at the target as a function of AK gap.

In these calculations as well as for the others discussed in this paper, we assume 100% charge and current neutralization in the gas cell. Recently, we have measured a maximum neutralization of about 95% on HERMES III. The effect of this net current is to slightly modify the simulated trajectories. Its effect depends on the distribution of the net current, which we do not model here. The return current associated with the net current, however, should flow along the axis of the cell, as this is the lowest inductance path. Thus, the effect of the finite net current will be to reduce the external current calculated for a given curvature of the beam.

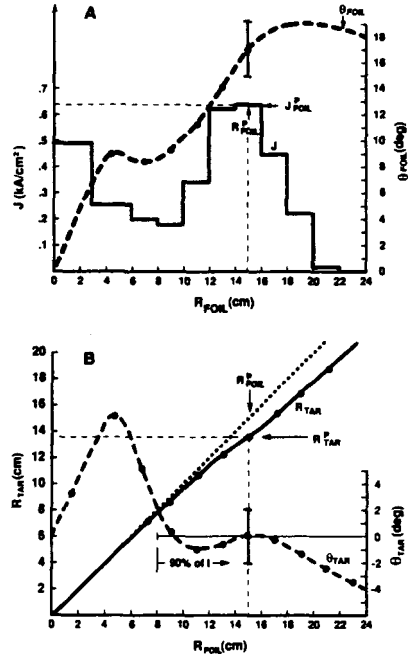

Figure 3(A). Current density and angle of incidence at conical foil corresponding to Figure 2A calculated as a function of radial position R(foil), and (B) Associated radial positions and angle of incidence at the target. Error bars refer to RMS deviation of angle at 15 cm.

TABLE 1

Characteristics of Electron Flow at the Conical Foil (Ti window) and at the target as a Function of AK Gap. See Section II and Figures 3 and 4 for definitions.

AK	R^P_{foil}	J^P_{foil}	θ^P_{foil}	$\bar{\theta}_{foil}$ $\pm$ RMS	I°	R^P_{TAR}
cm	cm	kA/cm^2	deg	deg	kA	cm
20	15	.64	17.1	15 $\pm$ 4.3	156	13.6
30	18	.44	15.6	13.5 $\pm$ 4.3	131	16.4
40	21	.32	13.7	11.6 $\pm$ 3.9	107	19.2

II. Radiation Pattern

We now turn to characterizing the radiation field as a function of the applied current in the lens. As we shall show, the diode with a 20-cm AK gap optimizes the radiation over an area of 1000 cm^2 at the target. For simplicity and for comparison with the radiation field obtained from a planar-anode diode optimized to produce radiation also over 1000 cm^2 (Figure 1), we restrict our simulations to compound-lens diodes with just the 20-cm gap. These simulations, together with

the general behavior of the flow shown in Table 1, however, permit the characteristics of the radiation field to be estimated for other AK gaps.

In the simulations, the steady state flow in the AK gap generated by MAGIC at 20 MV, together with the kinetic-energy distribution measured for HERMES III shot 396 (scaled to 20 MeV), was used as input to CYLTRAN. The target modeled was identical to that used to optimize the radiation fluence from HERMES III. The modeling was similar to that discussed in References 2 and 4, where additional details can be found.

In Figure 4A, the dose•area product over a 1000 cm^2 area and the ratio of the maximum to minimum dose over this area at the downstream target face are plotted as functions of external current. The radiation uniformity is optimized over the area when the external current equals about 156 kA. At this current, the dose•area is the same as that obtained from a planar-anode diode with 50-cm AK gap (Figure 1). For the planar-anode diode, the calculated maximum to minimum variation in dose over 1000 cm^2 is 2.2 to 1, which agrees well with measurements. For the compound-lens diode at 156 kA, the variation is only 1.4 to 1, which gives an improvement of a factor of 1.6 over that obtainable from the planar anode, while still maintaining the same dose•area product.

Figure 4B shows the variation in dose over the volume 1000 cm^2 x 15 cm as a function of external current. As with the variation at the front face, 156 kA minimizes the variation. At this minimum, the variation in dose over the volume is 2.5 to 1. For the 50-cm planar-anode diode, the corresponding calculated and measured variation is 6 to 1 and 5 to 1, respectively. Hence, the use of the lens should improve the radiation uniformity with depth by a factor of about 2.5.

As discussed in Section I, 156 kA corresponds to approximately paraxial trajectories at the target for a 20-cm AK gap. This condition, in addition to optimizing the uniformity of the near radiation field (Figures 4A and B) also approximately maximizes the far-field radiation dose (Figure 4C). At 156 kA, the axial dose 5.07-m downstream of the target is calculated to be factor of 3.3 higher than that obtainable from the 50-cm planar-anode diode.

Figure 5 summarizes the results of this section by showing the radiation field at the target and 15-cm downstream as calculated for the compound-lens diode operating with 156 kA. Note the significantly improved uniformity relative to that calculated for the planar-anode diode (Figure 1).

III. Design Considerations

Based on the simulations discussed in Sections I and II, we have designed the compound-lens diode shown in Figure 6. Initially, the same 6.4 kJ bank supply used to drive the B_θ-lens diode in the HELIA tests [4] will be used.

The cell is designed to operate with nitrogen gas at pressures near the minimum of the Paschen curve, in order to provide rapid charge and current neutralization of the incident beam. To help prevent the cell from flashing from the external voltage used to produce the lens current, the length of the insulator stack is maximized (24 cm). Additionally, a shield is placed internal to the cell to reduce illumination of

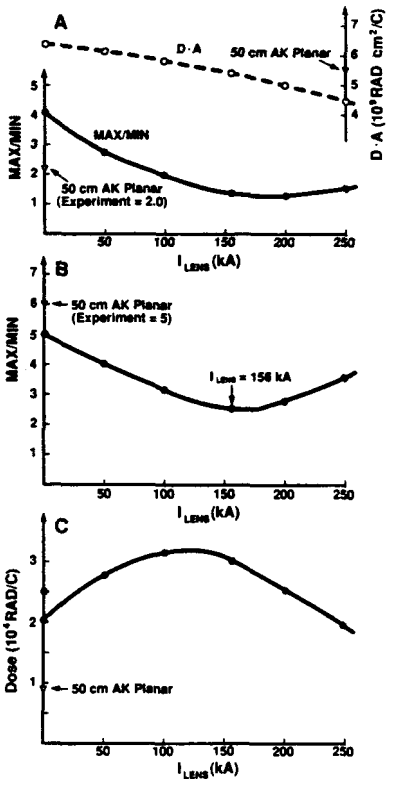

Figure 4(A). Dose•area product and variation (maximum to minimum) in dose over 1000 cm^2 area centered at downstream target face as a function of external current corresponding to geometry of Figure 2, (B) Associated variation in dose over the volume 1000 cm^2 x 15 cm defined by extending the area downstream by 15 cm, and (C) Associated axial dose 5.07-m downstream of target.

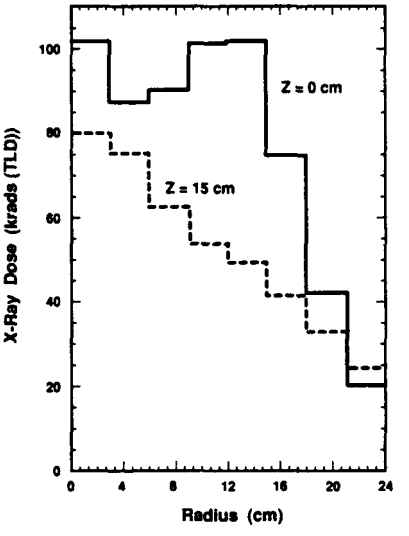

Figure 5. Radiation dose profile at target face and 15-cm downstream for compound-lens diode of Figure 2 with 156 kA assuming V(peak) = 18 MV and Q = 23.2 mC. Compare with Figure 1.

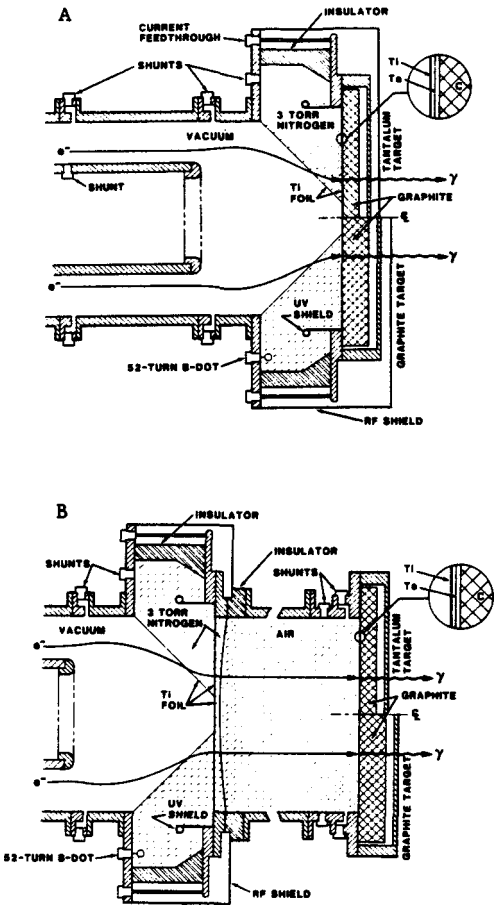

Figure 6. Schematic of (A) compound-lens diode and (B) compound-lens-injector drift-cell being constructed.

the stack by UV generated from plasma formation in the cell, which could initiate insulator flashover.

The entrance cone is made of a thin titanium foil (305 μm) to minimize the multiple-Coulomb-scattering ($\pm 5°$) of the incident beam and to minimize the likelihood of ion formation [7] and spallation.

Downstream of the gas cell, our existing graphite or optimized-tantalum bremsstrahlung targets [2] will be used. The construction is modular. This type of construction enables the beam to be incident on either target as well as permitting the beam to be injected into a gas cell as shown in Figure 6B. Short gas cells will be used for electron exposures. Long cells enable the beam to be transported over large distances for exposures in the alternate HERMES III test cell that is located outside the building. Calculations predict that by removing the coherent pinch angle before injection into such a cell, as can be done with the compound-lens, the beam can be made to propagate over large distances ($\gtrsim 10$ m) more efficiently [8].

Summary

Relative to a planar-anode diode, our calculations predict that the compound-lens diode is capable of providing significantly improved radiation uniformity. Assuming HERMES III to be operating at a peak voltage of 18 MV, our calculations predict that an average dose of 92 krads over 1000 cm^2, with a 1.4 to 1 uniformity over 1000 cm^2 and 2.5 to 1 uniformity over 1000 cm^2 x 15 cm can be generated with the lens. Increased AK gap and reduced lens current lead to reduced doses over larger areas. Moreover, changes in the radiation field are easily achieved by simple adjustments in the external current or gas pressure, thus avoiding the operational complexity and time consuming requirement of breaking vacuum for diode/target modifications. In addition, the lens relative to the planar-anode diode has the potential for generating higher doses in the far field and improved beam transport in long gas cells owing to reduced beam dispersion.

Based on the considerations presented in this paper, a diode has been designed (Figure 6) and should be ready for testing during the summer of 1989.

References

[1] J. J. Ramirez, K. R. Prestwich, J. A. Alexander, J. P. Corley, G. J. Denison, C. W. Huddle, D. L. Johnson, R. C. Pate, G. J. Weber, E. L. Burgess, R. A. Hamil, J. W. Poukey, T. W. L. Sanford, L. O. Seamons, G. A. Zawadzkas, I. D. Smith, P. W. Spence, and L. G. Schlitt, in Proceedings of 7th International Conference on High-Power Particle Beams, Karlsruhe, Germany, July 4-8, 1988, edited by Walter Bauer and Winfried Schmidt (Kernforschungszentrum, Karlsruhe GmbH, 1988), pp. 148-157.

[2] T. W. L. Sanford, J. A. Halbleib, J. W. Poukey, G. T. Baldwin, G. A. Carlson, W. A. Stygar, T. Sheridan, R. Mock, T. A. Borkey, G. W. Crowder, M. F. Current, H. C. Ives, G. A. Maston, R. C. Plate, G. Douglas, E. R. Brock, J. A. Alexander, C. O. Landron, P. W. Spence, V. L. Bailey, and H. Kishi, IBID., pp. 326-332.

[3] T. W. L. Sanford, J. A. Halbleib, J. W. Poukey, T. P. Wright, C. E. Heath, R. Mock, P. W. Spence, G. Proulx, V. Bailey, J. Fockler, and H. Kishi, Appl. Phys. Lett. 50, 809 (1987).

[4] T. W. L. Sanford, J. A. Halbleib, J. W. Poukey, C. E. Heath, R. Mock, V. Bailey, G. A. Proulx, P. W. Spence, and H. Kishi, Appl. Phys. Lett., Vol. 54, 1406 (1989).

[5] B. Goplen, R. E. Clark, J. McDonald, and W. M. Bollen, Mission Research Corporation Report No. MCR/WDC-R-068, 1983.

[6] J. A. Halbleib and T. A. Mehlhorn, Nucl. Sci. Eng. 92, 338 (1986).

[7] T. W. L. Sanford, J. A. Halbleib, J. W. Poukey, A. L. Pregenzer, R. C. Pate, C. E. Heath, R. Mock, G. A. Masten, D. C. Ghiglia, T. J. Roemer, P. W. Spence, and G. A. Proulx, Sandia National Laboratories Report No. SAND88-1297, 1988.

[8] D. Welch, Mission Research Corp., private communication, 1989.